The Number of Fades in Space-Diversity Reception

By ARVIDS VIGANTS

(Manuscript received February 11, 1970)

Experimental and theoretical results are presented which show that deep fades due to multipath propagation on line-of-sight microwave links are greatly reduced in number when two vertically separated receiving antennas are used and the stronger of the two received signals is selected as the diversity signal. The experimental results are based on 6 GHz propagation data obtained for a 72-day period on a 28.5 mile path in Ohio, with a 27.5 foot vertical separation of the receiving antennas. The theoretical results are obtained by treating the received signals as correlated Rayleigh distributed random variables. Theoretically predicted variations with fade depth agree with experimental observations. Combination of the theoretical results with experimentally determined parameters provides results which can be used, for example, to calculate the reduction in the number of fades as a function of the vertical separation of the receiving antennas, wavelength, path length, fade depth, and the gain difference (if any) of the receiving antennas.

I. INTRODUCTION

Line-of-sight microwave transmission is affected by a phenomenon called multipath propagation. When this phenomenon is present, the output from a receiving antenna can be practically zero for seconds at a time. However, such deep fades rarely occur simultaneously in the outputs of two vertically separated receiving antennas, and this is the basis for space-diversity reception on line-of-sight microwave links.

The number of fades and the average durations of fades are fundamental properties of the line-of-sight microwave channel. In high performance systems, they may determine the limit of attainable performance. Previous discussions of space diversity do not cover the number of fades and their average durations.[1-3] Experimental

data on these are difficult to obtain because long periods of time are needed to observe a number of fades sufficient for theoretical analysis. We present a set of experimental results obtained from measurements made in 1966 in Ohio. We also present, and this is a major part of the paper, theoretical results on the number of fades and their average durations.

The diversity scheme for which our results are obtained is one where the diversity signal is, at all instants of time, the stronger of two received signals. This scheme is of interest because of its inherent simplicity, and because experimental values for the diversity signal can be obtained easily during computer processing of experimental observations of the received signals. From a broader point of view, this provides information about simultaneous behavior of pairs of received signals that can be used in reliability and interference calculations, and in performance calculations for diversity schemes other than the simple one above.

The number of deep fades is greatly reduced when space-diversity reception is used. We show how to calculate this reduction as a function of the vertical separation of the two receiving antennas, wavelength, path length, depth of fade, and the gain difference (if any) of the receiving antennas. Our results are based on a combination of theory and experiment. The outputs of the receiving antennas during deep fades are treated as random variables that are jointly Rayleigh distributed.[4,5] This provides a description of how various quantities change with fade depth. Parameters describing the occurrence of fading, correlation in space, and the spectral width of the fluctuations are determined from experimental data.

The theoretical expressions describe our experimental observations quite well. However, both theoretical knowledge of fading and the amount of experimental data on fading are limited, and the theoretical model presented here may need modifications as work proceeds and more data become available.

II. EXPERIMENTAL RESULTS

The transmitted power in microwave line-of-sight communication systems is constant (angle modulation is used). Fading information can therefore be obtained from working systems, without interfering with their operation, by installing additional equipment to monitor the power output of the receiving antennas. This was done at West Unity, Ohio, where, in addition, two 8-foot diameter parabolic reflector antennas were installed below existing antennas to provide information

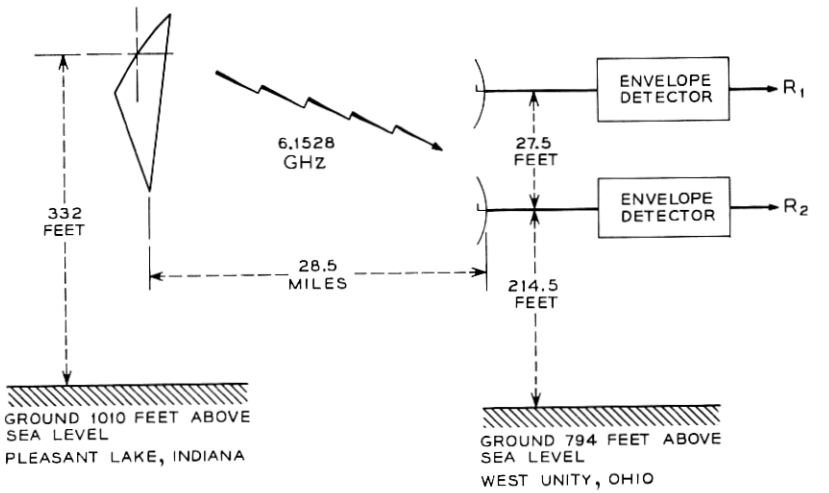

Fig. 1—Essential parameters of the experiment.

about space-diversity reception. We will discuss the fades observed on these two receiving antennas.

The microwave link on which the data were obtained is shown schematically in Fig. 1. The boxes labeled "envelope detector" represent rather sophisticated equipment used in the investigation of fading. The path length was 28.5 miles.* The transmitting antenna at Pleasant Lake, Indiana, was a standard system antenna—a 10-foot horn reflector. The center-to-center vertical separation of the receiving antennas was 27.5 feet. The basic experimental data consisted of observations of the envelopes of received angle-modulated signals centered on 6.1528 GHz.

An important feature of the experiment was long-term coverage. Deep fades are rare events, and the received power must be observed continuously for long periods of time to arrive at a sample of adequate size. Reliability of equipment must be high, and the subsequent processing of the data is a formidable task, even with a computer, because of the high data volume. The data discussed here cover a 72-day period, July 19, 1966, to September 29, 1966.

The power received by the two antennas was sampled essentially simultaneously every 0.2 seconds, converted to a decibel scale, and recorded in digital form for subsequent computer processing (in the

* Ground reflections were negligible, and transmission to the bottom antenna had a clearance of about 15 feet (over trees) at 2/3 earth radius conditions.

absence of fading the recording rate was less than the sampling rate). The quantizing steps in the analog-to-digital conversion were somewhat less than 2 dB, which represented a compromise between quantization error and the number of bits needed to encode the power levels (five bits were used). During computer processing, the power level at a sampling instant was assumed to hold until the next sampling instant.

The data were first processed to determine the received power levels on each antenna in the absence of fading. The received power levels during fading were then normalized to the corresponding power levels in the absence of fading. We denote by 20 log R_1 and 20 log R_2 the normalized dB readings from the top and the bottom receiving antennas respectively. The voltage envelope from the top antenna is R_1, and the voltage envelope from the bottom antenna is R_2. As a consequence of the normalization, both R_1 and R_2 are unity in the absence of fading.

The diversity signal was synthesized during processing by taking the stronger of the two received signals at each sampling instant. The envelope of the diversity signal is

$$R = \max (R_1, R_2). \tag{1}$$

The diversity signal is synthesized from signals that are quantized, and 20 log R can therefore have errors with an upper bound of roughly 2 dB.

A signal is said to be in a fade of depth L and duration τ when its voltage envelope (R_1, R_2, or R) becomes less than L and remains less than L for τ seconds. During processing, the number of fades of depth L were counted for a set of values of L, and the average fade durations were obtained by dividing the sum of the durations by the number of fades. We restrict our discussion to fades deeper than -20 dB; that is, to values of L that are less than a tenth.

The results for the average fade durations are shown in Fig. 2. (The two theoretical solid lines will be discussed later. The diversity points for fades close to -40 dB are not shown, because an average based on only three observations would not be meaningful.) The durations can be substantial. For example, the average fade duration of a nondiversity signal at -40 dB is about five seconds. Diversity does not reduce these durations appreciably. The reduction is roughly by a factor of two, which can be inferred from a simple heuristic argument as follows. Because the receiving antennas are not very far apart, the fade durations of R_1 and R_2 are roughly the same, but offset in time. As fades become deeper they become shorter, and the offsets start to exceed the fade durations, which results in a large reduction

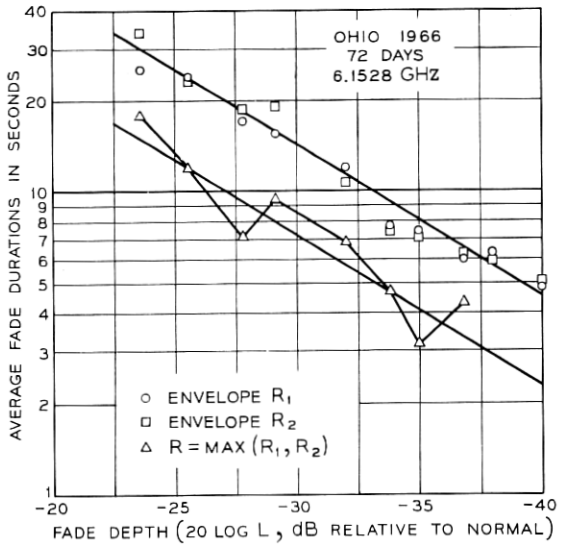

Fig. 2—Average fade durations (Ohio, 1966, 72 days, 6.1528 GHz—the two lines are theoretical).

in the number of deep simultaneous fades (we will see this shortly). Suppose both R_1 and R_2 undergo fades of duration τ. An overlap of the fades, if it does occur, has a value between 0 and τ. There is no preferred overlap position, and $(\tau/2)$ is therefore the average duration of a simultaneous fade.

The results for the number of fades in the 72-day period are shown in Fig. 3. Space diversity has been quite successful in reducing the number of fades. As a matter of fact, the reduction for the deeper fades is so large that the 72-day period was barely adequate for the observation of any -40 dB simultaneous fades at all. From the experimental points, the reduction at -40 dB is by about a factor of twenty. However, this is based on a small sample of only three simultaneous fades at -40 dB. The theoretical curves (discussed later) suggest that, on the average, the reduction at -40 dB will be by about a factor of sixty. There is a small systematic difference in the number of fades of R_1 and R_2. We hope to obtain more information on this from experiments now under way at Palmetto, Georgia.

The conclusion from these observations is that space diversity acts mostly by reducing the number of fades, and that the reduction increases as the fades become deeper.

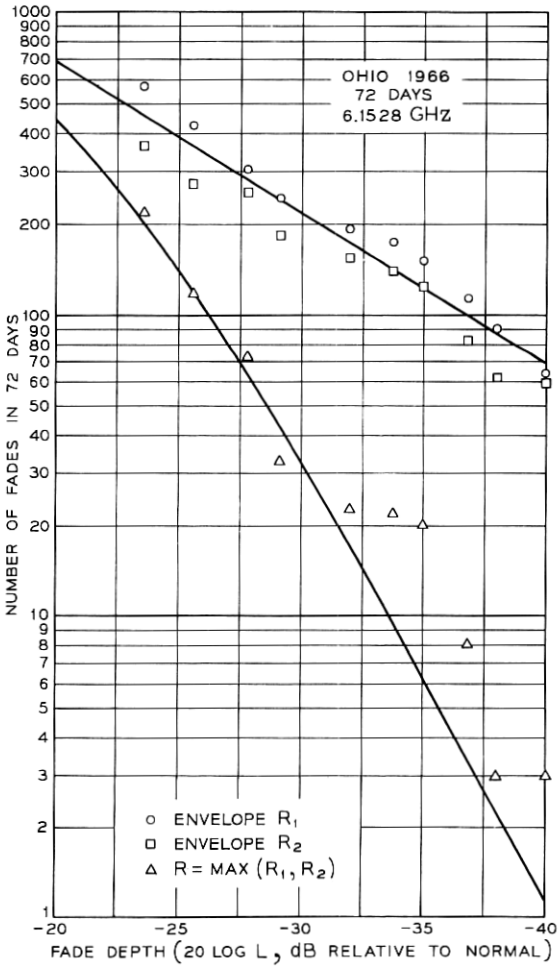

Fig. 3—Number of fades (Ohio, 1966, 72 days, 6.1528 GHz—the curves are theoretical).

III. THEORETICAL MODEL

The number of fades and the average fade durations vary with fade depth. The functional form of the variations can be calculated from probability theory, using methods developed by Rice,[4,5] if various probability density functions associated with R_1, R_2, and R are known.

To arrive at a set of probability density functions for the present

problem, we note that multipath fading normally occurs during relatively short intervals, separated by long periods that contain no fading. Let T_o denote the total time of observation (72 days in the case of the experimental data in the previous section), and let $T(R_1 < L)$ and $T(R_2 < L)$ denote the respective amounts of time during which R_1 and R_2 have values less than L. A mathematical description of experimental observations[3] of these times is

$$T(R_1 < L) = rT_0L^2, \qquad L < 0.1 \tag{2}$$

$$T(R_2 < L) = rT_0L^2, \qquad L < 0.1. \tag{3}$$

The parameter r is proportional to the ratio of time containing fading to total time. It is a function of the length of the line-of-sight path, frequency, time of the year (summer or winter), climate, and terrain.[6]

To introduce some generality, suppose that the gain associated with the bottom antenna is changed, so that the value of R_2 in the absence of fading changes from unity to a value v. If R_2 is still measured on the same scale as R_1 ,* then equation (3) becomes

$$T(R_2 < L) = rT_0(L/v)^2, \qquad (L/v) < 0.1. \tag{4}$$

The parameter v allows top and bottom antennas of different sizes (the gain difference in dB is 20 log v). If the bottom antenna is smaller than the top antenna, then v is less than unity. This is the case when a second antenna is added below a main antenna on an existing tower, and the size of the second antenna is limited by the allowable wind load on the tower.

The probabilities that R_1 and R_2 respectively are less than L are obtained by dividing $T(R_1 < L)$ and $T(R_2 < L)$ by a normalized time rT_o :

$$\begin{aligned} \Pr(R_1 < L) &= (rT_0)^{-1}T(R_1 < L) \\ &= L^2, \qquad L < 0.1 \end{aligned} \tag{5}$$

$$\begin{aligned} \Pr(R_2 < L) &= (rT_0)^{-1}T(R_2 < L) \\ &= (L/v)^2, \qquad (L/v) < 0.1. \end{aligned} \tag{6}$$

The basis of our theoretical description of fading is the observation that the Rayleigh probability distributions

$$\begin{aligned} \Pr(R_1 < L) &= 1 - \exp(-L^2) \\ &\cong L^2, \qquad L < 0.1 \end{aligned} \tag{7}$$

* Fade depths of all signals are expressed in decibels relative to the value of the received signal from the top antenna in the absence of fading.

$$\Pr(R_2 < L) = 1 - \exp(-L^2/v^2)$$
$$\cong (L/v)^2, \qquad (L/v) < 0.1 \tag{8}$$

have the same form as equations (5) and (6) for deep fades. This suggests that during deep fades pairs of received envelopes can be treated theoretically as correlated Rayleigh distributed variables. Note that in this theoretical model, as a consequence of equations (7) and (8), the mean square values of the envelopes are

$$\langle R_1^2 \rangle = 1, \qquad \langle R_2^2 \rangle = v^2 \tag{9}$$

where the angle brackets denote averages.

Given that R_1 and R_2 are jointly Rayleigh distributed, one can proceed purely theoretically and obtain expressions for the number of fades and the average fade durations of R. The general expressions for the number of fades are obtained in Appendix A. The probability density functions are listed in Appendix B. The theoretical results can be expected to apply only to deep fades because of the restrictions on L in equations (2) through (8). Reduction to the case of deep fades is carried out in Appendix C, and the results are summarized and discussed in Section IV.

IV. THEORETICAL RESULTS FOR DEEP FADES

The theoretical results for the number of fades and for the average fade durations become relatively simple when fades are deep. Deep in the context here means, first, that

$$L < 0.1, \qquad (L/v) < 0.1, \tag{10}$$

which is just a restatement of the conditions that appeared in the previous section. Second, there are associated conditions that come out of the mathematics in the appendices,

$$q^{-1}L^2 < 0.1, \qquad q^{-1}(L/v)^2 < 0.1. \tag{11}$$

The parameter q describes the correlation of R_1^2 and R_2^2. It is unity when the receiving antennas are very far apart, and it becomes zero when the two receiving antennas merge into one. We give an empirical expression for q when we compare the experimental and theoretical results in Section V. The conditions in equation (11) show how the separation of the receiving antennas affects the range of fade depths for which the simple approximations presented in this section are valid.

The number of fades of the diversity signal is one of the main results. For deep fades, the number of fades of R per unit time is

$$N \cong c(1 + v)(v^2q)^{-1}L^3, \tag{12}$$

where the parameter c is proportional to the rms value of the time derivative of R_1 ,

$$c = [(2/\pi)\langle(dR_1/dt)^2\rangle]^{\frac{1}{2}}. \tag{13}$$

The corresponding number of fades of the envelope R_1 per unit time is

$$N_1 \cong cL. \tag{14}$$

The reduction in the number of fades provided by diversity is therefore

$$\begin{aligned} F_N &= N_1/N \\ &\cong (1 + v)^{-1}v^2qL^{-2}, \end{aligned} \tag{15}$$

which can be a large number for deep fades (L close to zero).

Numerical estimates of F_N can be obtained using values of q given by equation (19) in Section V. For example, a vertical separation of the receiving antennas that often appears adequate is 40 feet.[1,2] For this, q is about 0.025 at 6 GHz on a 26.5 mile path, which is a typical average path length. For receiving antennas of equal size (v is unity), the reduction in the number of fades is (from equation (15)) about 125 at -40 dB. This means that at the -40 dB level there is, on the average, only one overlap in 125 fades of the nondiversity signals.

The expressions for various quantities, when fades are deep, are summarized in Table I, where the first column refers to R_1 and the second column to R. This shows that the average fade duration of R is

$$\langle t\rangle \cong (1 + v)^{-1}\langle t_1\rangle \tag{16}$$

where $\langle t_1\rangle$ is the average fade duration of R_1 . The ratio of $\langle t_1\rangle$ to $\langle t\rangle$ is independent of fade depth for deep fades, and it becomes two when v

TABLE I—EXPRESSIONS FOR VARIOUS QUANTITIES FOR DEEP FADES

	Nondiversity	Diversity	Improvement
Probability of fade	L^2	$(v^2q)^{-1}L^4$	v^2qL^{-2}
Number of fades	cL	$c(1 + v)(v^2q)^{-1}L^3$	$(1 + v)^{-1}v^2qL^{-2}$
Average duration	$c^{-1}L$	$c^{-1}(1 + v)^{-1}L$	$(1 + v)$

is unity (same size receiving antennas), which supports the heuristic argument given previously in the section on the experimental results.

The reduction in the total amount of time spent in fades is*, from the first row in Table I,

$$F \cong v^2 q L^{-2}. \tag{17}$$

Therefore

$$F_N \cong (1 + v)^{-1} F. \tag{18}$$

When v is unity or less, conditions (10) and (11) translate into a simple statement that the approximations presented here are valid when F is larger than ten.

V. COMPARISON OF EXPERIMENTAL AND THEORETICAL RESULTS

The theory predicts that the number of fades and the average fade durations are certain functions of the fade depth L. This can be verified experimentally. The theory also contains four parameters (r, v, q, c). One of these, the gain difference v, is a design parameter that we control. The other three (r for occurrence of fading, q for correlation in space, c for spectral width of fluctuations) depend on the inhomogeneities of the atmosphere and their interaction with electromagnetic waves. Since we do not know how to determine these parameters theoretically for deep fades on microwave line-of-sight links, we determine them from the experimental data.

In the experiment, the gain difference parameter v is unity. An empirical result[3] for the correlation parameter q is

$$q = (2.75)^{-1}(s^2/\lambda d), \tag{19}$$

where s is the vertical center-to-center separation of the receiving antennas, λ is the wavelength, and d is the path length—all measured in the same units. For the receiving antenna pair discussed here, the value of q is 0.012, which is one of the experimental values[3] on which equation (19) is based. The value of the fade occurrence parameter r is one-half (from Fig. 5 in our previous work[3]).

The theoretical description of the average fade durations of R_1 and R_2 in Fig. 2 is

$$\langle t_1 \rangle = c^{-1} L. \tag{20}$$

---

* We have discussed this previously.[3] The parameter q denotes the quantity $(1 - k^2)$ appearing in the earlier work and in Appendix B here.

Least squares fitting of equation (20) to the experimental points gives*

$$c \cong 2.22 \times 10^{-3} \text{ second}^{-1}. \tag{21}$$

The data are in good agreement with the theoretically predicted dependence on L to the first power. Theory also predicts that the average fade durations of the diversity signal should be shorter by a factor of two, and the corresponding theoretical line in Fig. 2 describes the experimental points quite well. The larger scatter in the diversity points is caused by the small number of observations of deep simultaneous fades.

The number of fades can now be calculated entirely from theory. The number of fades per unit time of the nondiversity signals is given by equation (14). The corresponding number of fades in 72 days is

$$N_1' = rT_0N_1 \cong 6.9 \times 10^3 L. \tag{22}$$

This equation, shown as the top solid line in Fig. 3, describes the data adequately. Similarly, the number of fades of the diversity signal envelope R in 72 days is, using (12),

$$N' = rT_0N \cong 1.15 \times 10^6 L^3. \tag{23}$$

The deep fade approximation in this case applies only to fades deeper than about -30 dB, and the curved section of the bottom solid curve in Fig. 3 was therefore computed from expressions in the appendices. The departures from the curve when the number of simultaneous fades becomes small are very likely statistical in nature. Similar curves for frequency diversity (to be published), where we have more than one set of data, show deviations both above and below the theoretical curves in apparently random fashion over fifteen sets of data. Furthermore, as discussed earlier, experimental values for 20 log L can be in error by up to about 2 dB because the diversity signal is synthesized from quantized signals.

---

* The parameter c is related to the spectral width of the fluctuations of R_1 (the spectra of R_1 and R_2 are assumed to differ only by a multiplicative constant, which allows the mean square values to be different). For example, for a Gaussian spectrum

$$w(f) = (2/\pi)^{\frac{1}{2}} f_b^{-1} \exp(-f^2/2f_b^2)$$

the mean square derivative is

$$\langle (dR_1/dt)^2 \rangle = (2\pi f_b)^2$$

which can be substituted into equation (13) to relate c to f_b. We do not have experimentally determined spectra. As a speculation, using the value for c from expression (21), we obtain

$$f_b \cong 4.5 \times 10^{-4} \text{ Hz}.$$

All in all, we think the theory describes the experimental data well. To describe the data we needed only one additional parameter, the spectral width parameter c, beyond those determined previously[3] from amplitude distributions. The theoretical model based on the joint Rayleigh probability distribution therefore appears to give a highly consistent description of deep fades on line-of-sight microwave links.

VI. CONCLUSIONS

The experimental and theoretical results presented here show that, for fading caused by multipath propagation, simultaneous deep fades on vertically separated receiving antennas can be practically nonexistent. Furthermore, the theoretical results enable one to describe quantitatively what is meant by practically nonexistent. From a more general point of view, a theoretical description of the output of the receiving antennas may help in modeling the disturbances in the electromagnetic waves incident upon the antennas, on which much remains to be done.

VII. ACKNOWLEDGMENT

We are indebted to W. T. Barnett for many useful discussions. The experimental data come from an experiment to which many people at Bell Telephone Laboratories contributed. In particular, the Multiple Input Data Acquisition System (MIDAS) was designed by G. A. Zimmerman, and the ideas and work of C. H. Menzel were essential to the processing of the data.

APPENDIX A

General Expressions for the Number of Fades

For the diversity signal envelope R, the number of fades of depth 20 log L dB is equal to the number of times R crosses L in an upward direction. Suppose that a time period T is divided into n intervals of length dt such that an interval contains either none or one of the upcrossings. Let m_1 be the number of intervals containing upcrossings made at instants in time when R is R_1, and let m_2 be the number of intervals containing upcrossings made when R is R_2. Then the quantities

$$P_1 = m_1/n, \qquad P_2 = m_2/n \tag{24}$$

are conditional probabilities (the conditions are stated in the next

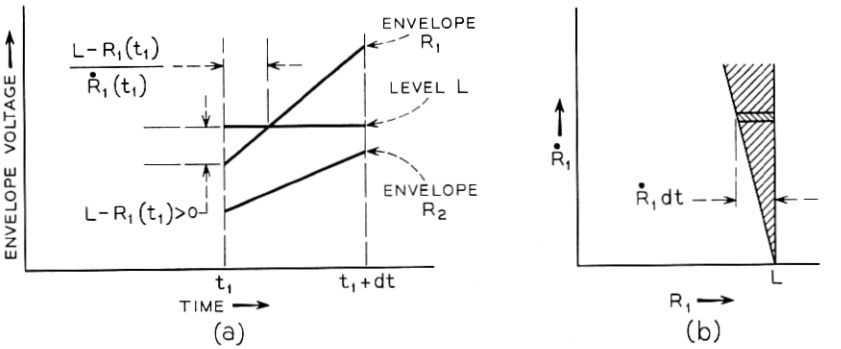

Fig. 4—Level crossing conditions: (a) level crossing in an interval of length dt, and (b) integration in the $(R_1, \dot{R}_1)$-plane.

paragraph) that R_1 and R_2 respectively cross a given level in an interval of length dt. The number of upcrossings of R per unit time is

$$N = (P_1 + P_2)/dt, \tag{25}$$

and the task is to express P_1 and P_2 in terms of the appropriate probability density functions.

To obtain an expression for P_1, we look in detail at an interval dt in which R_1 crosses a level L in an upward direction, as shown in Fig. 4. The interval length dt will go to zero in the limit, and the envelopes in the interval can therefore be represented by straight line segments. The conditions for the indicated level crossing to occur are*

$$R_2(t_1) < L \tag{26}$$

$$\dot{R}_1(t_1) > 0 \tag{27}$$

(the dot denotes a time derivative), and

$$0 < \frac{L - R_1(t_1)}{\dot{R}_1(t_1)} < dt. \tag{28}$$

Integration of the joint probability density function of $(R_1, R_2, \dot{R}_1)$ over the region in $(R_1, R_2, \dot{R}_1)$-space specified by the three inequalities will give the probability P_1. Let $p(R_1, R_2, \dot{R}_1)$ be this probability density. Then,

$$P_1 = \int_0^L dR_2 \int_0^\infty d\dot{R}_1 \int_{L-\dot{R}_1 dt}^L dR_1 p(R_1, R_2, \dot{R}_1) \tag{29}$$

* This approach follows Rice,[4] Section 3.3. The additional condition (26) comes in because we are treating a diversity signal.

where part (b) of Fig. 4 helps to visualize the integration with respect to R_1 as prescribed by the inequality (28). As dt approaches zero this becomes

$$P_1 = dt \int_0^L dR_2 \int_0^\infty d\dot{R}_1 \, \dot{R}_1 p(L, R_2 , \dot{R}_1). \tag{30}$$

The variables R_1 and $\dot{R}_1$ are uncorrelated (a random variable and its derivative are uncorrelated when measured at the same instant of time). If so, then to a good approximation R_2 and $\dot{R}_1$ are also uncorrelated, and*

$$p(R_1 , R_2 , \dot{R}_1) = p(R_1 , R_2)p(\dot{R}_1). \tag{31}$$

Therefore

$$P_1 = dt \int_0^\infty \dot{R}_1 p(\dot{R}_1) \, d\dot{R}_1 \int_0^L p(L, R_2) \, dR_2 . \tag{32}$$

The conditional probability P_2 can be obtained from this by an appropriate change of subscripts.

In terms of probability densities, the number of upcrossings of R per unit time is therefore

$$N = \int_0^\infty \dot{R}_1 p(\dot{R}_1) \, d\dot{R}_1 \int_0^L p(L, R_2) \, dR_2 + \int_0^\infty \dot{R}_2 p(\dot{R}_2) \, d\dot{R}_2 \int_0^L p(R_1 , L) \, dR_1 . \tag{33}$$

The number of upcrossings of R_1 per unit time can be obtained from the first term in N by extending the integration with respect to R_2 to infinity, which gives

$$N_1 = \left\{ \int_0^\infty \dot{R}_1 p(\dot{R}_1) \, d\dot{R}_1 \right\} p_1(L). \tag{34}$$

Similarly, the number of upcrossings of R_2 per unit time is

$$N_2 = \left\{ \int_0^\infty \dot{R}_2 p(\dot{R}_2) \, d\dot{R}_2 \right\} p_2(L). \tag{35}$$

Note that the probability density function of R at the value L is

* We are using the symbol p to denote probability density functions in general. The arguments of p specify the actual function.

$$\begin{aligned} p(L) &= (\partial/\partial L) \Pr (R < L) \\ &= (\partial/\partial L) \Pr (R_1 < L, R_2 < L) \\ &= (\partial/\partial L) \int_0^L dR_1 \int_0^L dR_2 p(R_1 , R_2) \\ &= \int_0^L p(R_1 , L)\, dR_1 + \int_0^L p(L, R_2)\, dR_2 . \end{aligned} \tag{36}$$

This shows that N can be expressed in the same form as N_1 and N_2 (a constant multiplied by a probability density function) only when the integrals with respect to $\dot{R}_1$ and $\dot{R}_2$ are equal; that is, when these integrals in equation (33) can be factored out.

The crossing rate N can be expressed in terms of the rates N_1 and N_2 . Combining equation (33), (34), and (35), we obtain

$$N = N_1 \Pr (R_2 < L \mid R_1 = L) + N_2 \Pr (R_1 < L \mid R_2 = L) \tag{37}$$

where $\Pr (R_2 < L \mid R_1 = L)$ is the probability that R_2 is less than L, subject to the condition that R_1 is equal to L, and similarly for the second term.

APPENDIX B

Probability Density Functions

To obtain the required probability density functions, the complex envelopes $[R_1 \exp (i\theta_1)]$ and $[R_2 \exp (i\theta_2)]$ are resolved into quadrature components

$$\left.\begin{aligned} x_1 &= R_1 \cos \theta_1 \\ x_2 &= R_2 \cos \theta_2 \\ x_3 &= \dot{x}_1 = \dot{R}_1 \cos \theta_1 - R_1 \dot{\theta}_1 \sin \theta_1 \\ y_1 &= R_1 \sin \theta_1 \\ y_2 &= R_2 \sin \theta_2 \\ y_3 &= \dot{y}_1 = \dot{R}_1 \sin \theta_1 + R_1 \dot{\theta}_1 \cos \theta_1 \end{aligned}\right\} \tag{38}$$

where the dot denotes a time derivative. The assumption that x_i and y_i $(i = 1, 2, 3)$ have zero means and are normally distributed with second moments

$$\langle x_n x_m \rangle = \langle y_n y_m \rangle = \lambda_{nm} , \qquad n, m = 1, 2, 3 \tag{39}$$

$$\langle x_n y_m \rangle = 0 \tag{40}$$

leads* to the Rayleigh probability density for R_1

$$p_1(R_1) = (R_1/\lambda_{11}) \exp(-R_1^2/2\lambda_{11}) \tag{41}$$

$$\langle R_1^2 \rangle = 2\lambda_{11} \tag{42}$$

with a similar form for the probability density function for R_2.

The probability density function of $\dot{R}_1$ can be obtained in a similar manner. The joint density function in this case is

$$\begin{aligned} p(\dot{R}_1, \dot{\theta}_1, R_1, \theta_1) &= R_1^2 p(x_1, x_3, y_1, y_3) \\ &= R_1^2 p(x_1)p(x_3)p(y_1)p(y_3) \\ &= \frac{R_1^2}{(2\pi)^2\lambda_{11}\lambda_{33}} \exp\left\{-\frac{x_1^2 + y_1^2}{2\lambda_{11}} - \frac{x_3^2 + y_3^2}{2\lambda_{33}}\right\} \\ &= \frac{R_1^2}{(2\pi)^2\lambda_{11}\lambda_{33}} \exp\left\{-\frac{R_1^2}{2\lambda_{11}} - \frac{\dot{R}_1^2 + R_1^2\dot{\theta}_1^2}{2\lambda_{33}}\right\}. \end{aligned} \tag{43}$$

Integration with respect to θ_1 (from 0 to 2π) and $\dot{\theta}_1$ (from $-\infty$ to ∞) gives

$$p(\dot{R}_1, R_1) = \frac{R_1}{\lambda_{11}(2\pi\lambda_{33})^{\frac{1}{2}}} \exp\left\{-\frac{R_1^2}{2\lambda_{11}} - \frac{\dot{R}_1^2}{2\lambda_{33}}\right\} \tag{44}$$

from which

$$p(\dot{R}_1) = (2\pi\lambda_{33})^{-\frac{1}{2}} \exp(-\dot{R}_1^2/2\lambda_{33}) \tag{45}$$

$$\langle \dot{R}_1^2 \rangle = \lambda_{33}. \tag{46}$$

It is interesting to note that $\dot{R}_1$ is normally distributed.

The joint probability density function of R_1 and R_2 is,[7] in our notation,

$$\begin{aligned} p(R_1, R_2) = (R_1R_2/q\lambda_{11}\lambda_{22}) \cdot \exp\{-(2q)^{-1}[(R_1^2/\lambda_{11}) + (R_2^2/\lambda_{22})]\} \\ I_0\{kR_1R_2/q(\lambda_{11}\lambda_{22})^{\frac{1}{2}}\} \end{aligned} \tag{47}$$

where I_0 is a modified Bessel function of the first kind, and

$$k^2 = \lambda_{12}^2/\lambda_{11}\lambda_{22} \tag{48}$$

$$q = 1 - k^2. \tag{49}$$

The conditional probability required in equation (37) is, therefore, from the probability density functions given above,

* Details can be found in Davenport and Root,[7] Section 8.5, where Rice's[4] work is summarized.

$$\Pr(R_2 < L \mid R_1 = L) = \int_0^L dR_2 p(L, R_2)/p_1(L)$$

$$= e^{-y} \int_0^x e^{-t} I_0[2(yt)^{\frac{1}{2}}]\, dt \tag{50}$$

where

$$x = q^{-1}(L^2/\langle R_2^2 \rangle) \tag{51}$$

$$y = q^{-1}k^2(L^2/\langle R_1^2 \rangle). \tag{52}$$

The other conditional probability $\Pr(R_1 < L \mid R_2 = L)$ can be obtained from these equations by appropriate changes of subscripts.

APPENDIX C

Deep Fade Approximations

For deep fades (small values of L) simple approximations of the various expressions can be obtained. First of all,

$$p_1(L) \cong 2L/\langle R_1^2 \rangle, \qquad (L/R_{1\,\mathrm{rms}}) < 0.1 \tag{53}$$

which immediately leads to

$$N_1 \cong c(L/R_{1\,\mathrm{rms}}), \qquad (L/R_{1\,\mathrm{rms}}) < 0.1, \tag{54}$$

where

$$c = \{(2/\pi)(\langle \dot{R}_1^2 \rangle/\langle R_1^2 \rangle)\}^{\frac{1}{2}}. \tag{55}$$

The envelope fluctuations can be assumed to fulfill the condition

$$\langle \dot{R}_1^2 \rangle/\langle R_1^2 \rangle = \langle \dot{R}_2^2 \rangle/\langle R_2^2 \rangle. \tag{56}$$

If so, then

$$N_2 = c(L/R_{2\,\mathrm{rms}}), \qquad (L/R_{2\,\mathrm{rms}}) < 0.1. \tag{57}$$

Now that the definitions are clear, we can start using the normalized mean square values

$$\langle R_1^2 \rangle = 1, \qquad \langle R_2^2 \rangle = v^2. \tag{58}$$

In terms of these,

$$N \cong cL\{\Pr(R_2 < L \mid R_1 = L) + v^{-1} \Pr(R_1 < L \mid R_2 = L)\}. \tag{59}$$

When

$$q^{-1}L^2 < 0.1, \qquad q^{-1}(L^2/v^2) < 0.1, \tag{60}$$

the conditional probabilities become

$$\Pr(R_2 < L \mid R_1 = L) \cong q^{-1}(L^2/v^2) \tag{61}$$

$$\Pr(R_1 < L \mid R_2 = L) \cong q^{-1}L^2 \tag{62}$$

and

$$N \cong cq^{-1}v^{-2}(1 + v)L^3. \tag{63}$$

The average fade durations of the envelopes R and R_1 are, respectively,

$$\langle t \rangle = N^{-1} \Pr(R_1 < L, R_2 < L) \tag{64}$$

$$\langle t_1 \rangle = N_1^{-1} \Pr(R_1 < L). \tag{65}$$

Deep fade approximations of the probabilities are

$$\Pr(R_1 < L, R_2 < L) \cong q^{-1}v^{-2}L^4 \tag{66}$$

$$\Pr(R_1 < L) \cong L^2, \tag{67}$$

and appropriate substitutions into equations (64) and (65) provide the expressions in Table I.

In cases where the deep fade approximations do not apply, we evaluated the various integrals numerically. It is possible (but we did not do this) to use tables for the conditional probability, equation (50), since it can be expressed in terms of Marcum Q functions[8,9] that occur in communication theory. Similar integrals are denoted by $J(x, y)$ by Luke,[10] who gives references to tables that have to do with hitting a circular target (we could not obtain these tables).

REFERENCES

1. Makino, H., and Morita, K., "The Space Diversity Reception and Transmission Systems for Line-of-Sight Microwave Link," Rev. Elec. Commun. Lab. (Japan), *13*, (January-February 1965), pp. 111–129; also "Design of Space Diversity Receiving and Transmitting Systems of Line-of Sight Microwave Links," IEEE Trans. Commun. Tech., *COM-15*, No. 2 (August 1967), pp. 603–614.
2. White, R. F., "Space Diversity on Line-of-Sight Microwave Systems," IEEE Trans. Commun. Tech., *COM-16*, No. 1 (February 1968), pp. 119–133.
3. Vigants, A., "Space Diversity Performance as a Function of Antenna Separation" IEEE Trans. Commun. Tech., *COM-16*, No. 6 (December 1968), pp. 831–836.
4. Rice, S. O., "Mathematical Analysis of Random Noise," B.S.T.J., *23*, No. 31 (July 1944), pp. 282–332, and *24*, No. 1 (January 1945), pp. 46–156.
5. Rice, S. O., "Distribution of the Duration of Fades in Radio Transmission: Gaussian Noise Model," B.S.T.J., *37*, No. 3 (May 1958), pp. 581–635.
6. Barnett, W. T., "Occurrence of Selective Fading as a Function of Path Length, Frequency, and Geography," 1969 USNC/URSI Spring Meeting, April 21–24, 1969, Washington, D. C.
7. Davenport, W. B., and Root, W. L., *An Introduction to the Theory of Random Signals and Noise*, New York: McGraw-Hill, 1958, Section 8.5.
8. Marcum, J. I., *Table of Q Functions*, Rand Corporation, January 1, 1950.
9. Schwartz, M., Bennett, W. R., and Stein, S., *Communication Systems and Techniques*, New York: McGraw-Hill, 1966, Appendix A.
10. Luke, Y. L., *Integrals of Bessel Functions*, New York: McGraw-Hill, 1962, Chapter 12.